

Upgrading of Nondewatered Nondemetallized Lignocellulosic Biocrude from Hydrothermal Liquefaction Using Supercritical Carbon Dioxide

Montesantos, Nikos; Nielsen, Rudi P.; Maschietti, Marco

Published in:
Industrial & Engineering Chemistry Research

DOI (link to publication from Publisher):
[10.1021/acs.iecr.9b06889](https://doi.org/10.1021/acs.iecr.9b06889)

Publication date:
2020

Document Version
Accepted author manuscript, peer reviewed version

[Link to publication from Aalborg University](#)

Citation for published version (APA):
Montesantos, N., Nielsen, R. P., & Maschietti, M. (2020). Upgrading of Nondewatered Nondemetallized Lignocellulosic Biocrude from Hydrothermal Liquefaction Using Supercritical Carbon Dioxide. *Industrial & Engineering Chemistry Research*, 59(13), 6141-6153. <https://doi.org/10.1021/acs.iecr.9b06889>

General rights

Copyright and moral rights for the publications made accessible in the public portal are retained by the authors and/or other copyright owners and it is a condition of accessing publications that users recognise and abide by the legal requirements associated with these rights.

- Users may download and print one copy of any publication from the public portal for the purpose of private study or research.
- You may not further distribute the material or use it for any profit-making activity or commercial gain
- You may freely distribute the URL identifying the publication in the public portal -

Take down policy

If you believe that this document breaches copyright please contact us at vbn@aub.aau.dk providing details, and we will remove access to the work immediately and investigate your claim.

Upgrading of non-dewatered non-demetalized lignocellulosic bio-crude from hydrothermal liquefaction using supercritical carbon dioxide

Nikolaos Montesantos, Rudi P. Nielsen, Marco Maschietti*

Department of Chemistry and Bioscience, Aalborg University, Niels Bohrs Vej 8A, 6700, Esbjerg, Denmark

* E-mail: marco@bio.aau.dk

Abstract

Supercritical carbon dioxide (sCO₂) extraction was applied on a raw bio-crude, obtained by hydrothermal liquefaction of pinewood. The extractions were carried out in semicontinuous mode, in the range 80 to 150 °C and 330 to 450 bar. Extraction yields from 44 to 53 wt% were achieved. The extracts were richer in lower molecular weight (MW) compounds, with fatty acids and aromatic hydrocarbons concentrated up to 14 and 24 wt%, respectively. For comparable MWs, lower polarity compounds concentrated in the extracts. Compared to the feed, the extracts exhibited lower density (from 1030 kg/m³ down to 914 kg/m³), lower water content (from 5.7 wt% down to 1.3 wt%) and lower oxygen content (from 10.0 wt% down to 5.0 wt%). In addition, the metal content was drastically reduced (from 8500 mg/kg down to 170 mg/kg on average). In the context of biofuel production, the sCO₂ extracts are a better feed for catalytic hydrotreating.

1. Introduction

Hydrothermal liquefaction (HTL) is a promising thermochemical process to produce liquid fuel from biomass. The process entails the depolymerisation of biomass in an aqueous medium at high temperature (e.g. 250 – 450 °C) and pressure (e.g. 100 – 350 bar).¹ One of the major advantages of HTL involves the flexibility of feedstocks that can be processed, which include both dry and wet biomasses.² The utilization of lignocellulosic biomass, an example of so-called second generation biomass, is particularly appealing due to lack of direct competition with food production. Wood residue and excess lignin from the paper pulp industry are examples of lignocellulosic by-products produced in large quantities, which can be valorised to liquid fuels via HTL.^{3–5}

Besides the water medium, the HTL process is typically carried out in the presence of homogeneous catalysts and pH adjusters, such as potassium carbonate (K_2CO_3), sodium carbonate (Na_2CO_3), and sodium hydroxide (NaOH).^{1,6} The main products of HTL are a CO_2 -rich gas phase (typically around 90 wt% CO_2),^{7,8} a solid phase (i.e. char) and two liquid phases. The liquid products are an aqueous phase saturated of water-soluble organics and an oil, namely the HTL bio-crude.¹

The HTL bio-crude obtained by gravimetric separation of the products is a tight water-in-oil emulsion, with water content in the range 5 to 15 wt%.^{9–12} Typical ash content values are reported broadly ranging from 0.01 wt% up to 5 wt%.^{4,10,13} Individual values of the content of alkali and earth metals (e.g. potassium and iron) are typically not reported, except for a few cases.^{3,4} In comparison to fossil crude oils, HTL bio-crudes have relatively high oxygen content, typically in the range 10 to 20 wt%.^{10,12,14,15} The high oxygen content is caused by a variety of oxygenated components, such as ketones, fatty acids and different one-ring phenols (e.g. phenol, guaiacols, catechols). Moreover, oxygen is also expected to be contained in a complex large fraction of high boiling components,

41 including phenolic oligomers derived from the lignin fraction.¹⁶ The presence of a relatively large
42 heavy fraction, essentially non-volatile, is evident from previous works reporting vacuum distillation of
43 lignocellulosic HTL bio-crudes. It was observed that approximately 50 wt% of the oil cannot be
44 distilled even at very high vacuum (i.e. 1.3 mbar) at temperatures between 130 °C and 160 °C. The
45 atmospheric equivalent boiling point of this heavy fraction was above 400 °C.^{17,18} In the reported
46 distillation experiments, the bio-crude was dewatered prior the process, since the presence of water
47 would reduce the distillation efficiency, result to unsteady boiling and create control issues.¹⁷ In
48 addition to the above, HTL lignocellulosic bio-crudes have high viscosity (typically in the range 10^3 to
49 10^6 cP)^{19–21} and high density (typically above 1000 kg/m^3)^{5,7,20,22}.

50 In order to utilize HTL bio-crudes as drop-in biofuels, the oxygen content has to be drastically reduced.
51 The state of the art method for this purpose is catalytic hydrotreating (i.e. hydrodeoxygenation,
52 HDO).²³ However, hydrotreating of raw HTL bio-crudes can lead to accelerated deactivation of the
53 catalytic bed due to high metal content, which originates from the alkali catalysts used in the HTL
54 process and, to some extent, from the biomass itself.^{21,24} These metals deposit on the active sites of the
55 catalyst and promote sintering during catalyst regeneration.²⁵ Both of these mechanisms are
56 irreversible. Even at low concentrations, metals can drastically reduce the lifetime of the catalyst,
57 which needs to be replaced when the deposition of 3 – 4 wt% of metals is reached.²⁶ In addition, water
58 can reduce catalyst activity by modifying its surface or the pore structure.²⁵ Less water and oxygen in
59 the HDO feed is therefore beneficial due to the lower hydrogen requirement of the process and the
60 lower amount of water in the HDO reactor. In addition, reduced density values for the bio-crude are
61 desirable in order to increase the drop-in potential with different types of petroleum fuels, such as
62 kerosene (775 to 840 kg/m^3),²⁷ diesel (820 to 845 kg/m^3)²⁸ and marine fuels (up to 991 kg/m^3).²⁹

63 The application of a separation process upstream the hydrotreating, aimed at obtaining a large fraction
64 of HTL bio-crude exhibiting favourable properties for the hydrotreating process itself (especially low
65 water, oxygen and metal content), is worth analysing. Among alternative separation processes,
66 supercritical carbon dioxide (sCO₂) extraction is appealing for a number of reasons: i) it is an
67 environmentally friendly process, thus suitable by nature for the sustainability paradigm that should
68 characterize biofuel production; ii) CO₂ is internally generated in the HTL process; iii) it is a process
69 competitive to distillation in the presence of high boiling point oils, as temperatures required in
70 distillation may be too high even at high vacuum.³⁰ The separation of high boiling point liquid mixtures
71 using sCO₂ is at industrial level for the fractionation of perfluoropolyether oligomers³¹ and it has been
72 applied at pilot or demonstration scale in a number of cases. Some representative examples include the
73 separation of fish oil ethyl esters,^{32,33} or the removal of fatty acids from rice bran oil,³⁴ wheat germ oil³⁵
74 and olive oil deodorizer distillate.³⁶

75 In previous works, sCO₂ was reported capable of extracting a large fraction of a dewatered and
76 demetalized lignocellulosic bio-crude (extraction yields up to 49 wt%).^{22,37} The procedure used for the
77 dewatering and demetalization of the bio-crude used in the mentioned previous works^{22,37} is based on
78 dilution of the bio-crude in methyl ethyl ketone followed by washing in citric acid aqueous solutions.
79 Details on the procedure are available in the PhD Thesis of Jensen.³⁸ The previous works^{22,37}
80 demonstrated problem-free operation above 80 °C (i.e. 80 – 120 °C), while the extractions were not
81 smooth and sometimes characterized by equipment clogging at 40 °C and 60 °C. The only other works
82 found on extraction of lignocellulosic bio-crudes refer to pyrolysis oils, where the extracts
83 demonstrated lower viscosity,³⁹ and lower water content than the corresponding feeds.^{40,41}

The aim of this work is to assess the sCO₂ extraction process on a raw HTL bio-crude, which is to say a non-dewatered non-demetalized bio-crude obtained by gravimetric separation downstream the HTL reactor and without any further treatment. The specific objective of this work is therefore to assess the potential of sCO₂ extraction in carrying out dewatering, demetalization and bio-crude separation in a single process step, as well as to compare the characteristics of the sCO₂ separation on this raw bio-crude with the separation reported in previous works referring to a dewatered and demetalized bio-crude^{22,37}. In addition, the tested operating conditions were expanded to higher pressures (up to 450 bar) and temperatures (up to 150 °C), as the previous works^{22,37} indicated a positive effect with increasing these parameters. Extraction temperatures below 80 °C were instead not considered, due to the above-mentioned operating problems.

2. Materials and methods

2.1. Materials

2.1.1. Feed bio-crude

The feed HTL bio-crude was produced by continuous-flow hydrothermal liquefaction of pinewood at 400 °C and 300 bar using potassium carbonate as a catalyst and sodium hydroxide for pH adjustment, as previously reported in the literature.²² Details on the effect of the operating parameters on the hydrothermal liquefaction process can be found in the work of Jensen et al.⁶ As a difference compared to the previous work where sCO₂ was used to fractionate the bio-crude obtained in this thermochemical process, in the present work the bio-crude underwent neither dewatering nor demetalization. Therefore, it is a raw bio-crude simply obtained by gravimetric separation from the aqueous phase downstream of the HTL reactor. It appears as a black high-viscosity liquid (Figure 1a), even though less viscous than

the bio-crude of the previous work,²² and as a stable emulsion of water in oil, since no phase separation was observed during 6 months of storage.

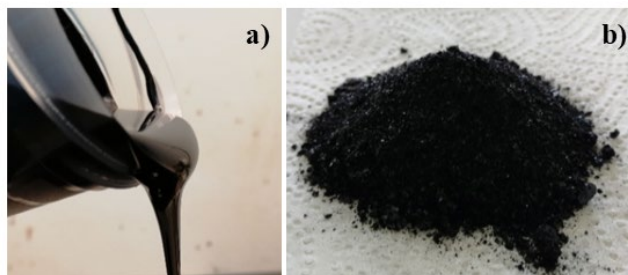


Figure 1. a) The HTL bio-crude used in this work; b) Example of the residue after sCO₂ extraction, tetrahydrofuran evaporation and mortar grinding. The example refers to the run at 450 bar and 100 °C.

2.1.2. Chemicals

Carbon dioxide (CO₂, 99.7 %) used for the supercritical extractions was purchased from Air Liquide (Denmark). Diethyl ether (DEE, 99 %) from VWR and pyridine (ACS grade) from Hach were used as solvents for the GC-MS analysis, while vanillin (99.8 %) and myristic acid (99 %) from Sigma Aldrich were used as internal standards. N,O-Bis(trimethylsilyl)trifluoroacetamide (BSTFA, 98.5 %) from Sigma Aldrich was used to derivatize samples. HYDRANAL Titrant 2 and Solvent oil from Fluka, as well as the Aquastar 1 % standard from Merck were used for the Karl Fischer titrations (KF). The elemental analyser was calibrated with the PerkinElmer Cystine 4G powder. Tetrahydrofuran (THF, 99.9 %) from VWR was used as solvent for retrieving the residue inside the sCO₂ extractor at the end of each extraction. Ethylene glycol (glycol, 98%) from VWR was used to prepare the aqueous solution (1:1 by mass) employed as cooling fluid in the cold trap described in Section 2.2. Tetrabutylammonium-hydroxide (TBAOH) 0.1 M in 2-propanol/methanol from Merck and tetraethyl ammonium bromide (TEABr) 0.4 M in ethylene glycol (Metrohm) were used as titrant and electrode electrolyte for

the total acid number (TAN) measurements. Toluene (99.5 %) and 2-propanol (99.8 %) from VWR were used as solvents for the TAN measurements. NIST traceable Metrohm buffers (i.e. pH 4, 7, 9) were used for calibration of the TAN electrode. Methyl ethyl ketone (MEK, 99 %) and methyl isobutyl ketone (MIBK, 99 %) from VWR, as well as THF, were used as solvents to estimate the density of the bio-crude. A 7 M nitric acid aqueous solution was used for acid digestion and the PlasmaCAL multi-element standard from SCP Science was used for the calibration of the ICP-OES instrument.

2.2. Supercritical CO₂ Extraction

The experimental setup was described in detail in a previous publication.²² Therefore, only a short description of the setup and the experimental method used in this work, together with notes about modifications, is provided here. The apparatus consists of a high-pressure extraction vessel (i.e. the extractor) with a 178 cm³ basket insert, where approximately 50 g of bio-crude were charged prior to an extraction. The basket insert was packed with 6 mm soda-lime glass beads up to approximately 1/3 of its height. The glass beads were chosen as an inert packing material that can disperse the bio-crude feed and improve its contact with the flowing sCO₂. A cylindrical filter (pore size 10 µm) is used at the top of the basket in order to prevent entrainment of particles. An automatically controlled heating jacket maintained the extraction temperature, which in this work was in the range 80 to 150 °C. The temperature indication was within ± 0.5 °C of the set value in all extractions. Liquid CO₂ from a dip-tube cylinder was subcooled by means of a heat exchanger fed with cold water (approx. 5 °C), which was provided by a thermostatic bath (Braun Frigomix U) and erogated by an immersion circulator (Julabo ED). Subsequently the CO₂ was compressed by a high-pressure pneumatic pump and fed to the entry port at the bottom of the extractor. The extraction pressure and the solvent flow rate were regulated manually by the pressure of the air supply of the pump and by a micrometering valve

145 downstream the extractor. The extraction pressures selected for this study were 330 bar and 450 bar. At
146 the tested conditions the extractions were smooth, with pressure gauge readings within ± 3 bar of the
147 set value in all runs. The micrometering valve was heated by hot air. The extract was collected in a 20
148 ml sampling vial inserted in a washing bottle immersed in a cold bath that was kept at approximately -
149 10 °C by means of a refrigerating circulator (Lab Companion RW3-0525P). A subsequent gas-washing
150 bottle immersed in the cold bath was packed with 3 – 4 g of cotton wool and aimed at collecting any
151 further condensate, or retaining fine droplets or particles that might be entrained with the CO₂, in order
152 to protect the downstream gas meter. The cotton wool was weighed after each extraction to account in
153 the mass balance. The weight difference of the cotton before and after an extraction was on average 0.1
154 g, while there was no condensate observed in the corresponding gas washing bottle. The gas meter
155 (Ritter TG3, max flow: 6 L/min; min flow: 0.1 L/min; accuracy: 0.5 %) measured the volume of CO₂
156 flowing through it and was equipped with a thermometer for measuring the gas temperature. The CO₂
157 flow rate in this work was in the range 3 to 4 L/min at gas meter conditions, corresponding to mass
158 flow rates in the range 4 to 6 g/min. After the completion of each extraction, the apparatus was
159 depressurized and let to cool down to about 80 °C, the basket insert dismounted and washed with 100 –
160 150 mL of THF in order to retrieve the residue. Preliminary tests showed that allowing the system to
161 cool down to ambient temperature was unfeasible, since the residue solidified incorporating the glass
162 beads and making its own retrieval problematic even with large amounts of THF. The drawback of the
163 recovery of the residue at 80 °C consisted in THF evaporation, together with losses of water contained
164 in the residue, which increased the uncertainty in the mass balance of water, as discussed in Section 3.
165 For extraction D (see Section 3.2), a small sample (approx. 1 g) of the mixture THF + residue was
166 saved for KF analysis, prior to solvent evaporation. THF was then separated from the residue by rotary
167 vacuum evaporation at 50 °C. The amount of THF in the mixture was estimated by subtracting the

mass of the residue after evaporation from the mixture THF + residue before evaporation. After the evaporation of THF, the residue appeared as a dry solid. It was ground in a mortar to obtain a fine powder (Figure 1b) and to ensure representative sampling for analysis.

2.3. Analytical characterization

2.3.1. Elemental analysis

Elemental analysis (EA) was performed with a PerkinElmer 2400 Series II CHNS/O analyser coupled with a PerkinElmer AD-6 Autobalance. Carbon, hydrogen and nitrogen were measured while oxygen was calculated by difference. Sulphur was in all measurements under the detection limit of the instrument and was omitted, since it is not expected to be present in this type of bio-crude. The instrument was calibrated by the Cystine standard (single point calibration) prior to each series of measurements, which were performed at least in triplicate. The Absolute Relative Deviation (ARD) between the measured elemental mass fractions of the standard compared to the theoretical values for C, H, and N was on average 0.4 %. The Relative Standard Deviation (RSD) on oxygen was 17 % for the feed bio-crude, whereas it was on average 21 % for the extracts and 6.4 % for the residues.

2.3.2. Water content

A Metrohm 870 KF Titrino Plus, coupled with a Metrohm 860 KF Thermoprep, was used for the KF water determination. The instrument was calibrated regularly with the Aquastar 1 % standard, as well as controlled with the standard prior to daily measurements. The ARD between the measured mass fraction of water of the standard and its theoretical value was always below 3 %. Approximately 0.1 g of bio-crude, extracts and residue (after solvent evaporation) were analysed. A sample of approximately 0.1 g was titrated also for the residue + THF mixture sample, in the case of Extraction D

(see Section 3.2). In this case, however, also the pure THF used for retrieving the residue was titrated in order to account for water already contained in the solvent. All KF measurements were performed at least in triplicate. The RSD for the feed bio-crude was 4.9 %, whereas it was on average 4.8 % for the extracts and 1.4 % for the residues.

2.3.3. Acid number measurements

The acid number measurements were carried out by potentiometric titration on a Metrohm Titrand 888 equipped with a Metrohm Solvotrode, following a procedure based on a modification of ASTM D664 test method B, which was developed in a previous work.²² The titration solvent was a mixture of toluene, 2-propanol and demineralized water (100:99:0.5, by volume), instead of pure 2-propanol,⁴² as this mixture proved more effective in dissolving the bio-crude and its extracts of this work. Approximately 0.1 g of bio-crude, extract or residue were diluted in 50 ml of the titration solvent and titrated. The method allows for determination of two acid numbers: the carboxylic acid number (CAN) and the total acid number (TAN), both expressed as mg KOH/g. The difference between TAN and CAN is the acid number that corresponds to the phenolic nature of acidity (PhAN), which is an important factor in lignocellulosic bio-crudes. The electrode was calibrated with 3 NIST traceable buffers (i.e. pH 4, 7, 9) and the calibration always demonstrated an R-squared (R^2) of at least 0.999 between pH and the measured electrical potential. According to the method, two inflection points are observed during the titration, which correspond to CAN and TAN, respectively. All TAN measurements were performed at least in triplicate. The RSD on TAN, CAN and PhAN for the feed bio-crude was 2.1 %, 1.4 % and 2.9 %, respectively. The average RSD on TAN, CAN and PhAN for the extracts was 1.6 %, 1.0 % and 1.6 %, respectively. The average RSD on TAN, CAN and PhAN for the residues was 1.3 %, 0.8 % and 1.0 %, respectively.

2.3.4. Density measurement

The density measurements were performed following a procedure developed before.²² The bio-crude density was measured with an Anton Parr DMA 35 Ex densitometer after dilution in three solvents (THF, MIBK and MEK), 1:1 by mass in each. Due to the small quantity of the sCO₂ extracts, their density was calculated by accurately measuring the mass of a volume displaced by a precision pipette (Gilson Microman M1000). The mass was weighed on an analytical balance (OHAUS PA224C) and the capillary piston used for each measurement was calibrated with distilled water in order to calculate accurately the displaced volume. The relative standard deviation (RSD) of triplicate pipetting of distilled water was always lower than 1 %. Density of pure water at the laboratory ambient conditions was taken from NIST.⁴³ All density measurements were performed in triplicate. The RSD for the feed bio-crude was 0.9 %, whereas it was on average 1.4 % for the extracts.

2.3.5. Metal content determination by ICP-OES

The metal content of the feed and of all the extracts, together with the metal content of the residue of selected extractions, was determined by Inductively Coupled Plasma - Optical Emission Spectrometry (ICP-OES), utilizing a PerkinElmer Optima 8000 system. The content of Potassium (K) and Sodium (Na) was measured, since they were expected due to the use of K₂CO₃ as catalyst and NaOH as pH adjuster in the HTL process. Additional metals subjected to quantitation were Aluminium (Al), Iron (Fe), Magnesium (Mg) and Titanium (Ti), since they are expected to derive from wear of equipment and natural presence in the pinewood biomass.²⁴ Samples were prepared by acid digestion and dilution. Approximately 0.5 g of sample were digested in an autoclave in 20 ml of 7 M aqueous nitric acid for 30 minutes at 120 °C and 2 bar. A blank of the nitric acid solution was digested as well for each set of samples and non-zero concentrations were subtracted from the sample measurement in order to account

for baseline errors. The digested samples were diluted with distilled water in a volumetric flask (Class A), and filtered by filter paper (pore size 4-12 μm). Dilution to 50 ml was performed for the bio-crude and the residues, while dilution to 25 ml was applied for the extracts. In case of visually observed turbidity of the solution, which was assumed to be due to organic particles, a second filtration was performed to acquire a transparent fluid to protect the plasma torch. In order to ascertain the reproducibility of the sample preparation procedure, eight samples of different mass of the feed bio-crude (i.e. 0.4 to 1 g) were digested and analyzed. The extracts and residues were measured in duplicate. The standards solutions used for calibration were prepared by diluting the PlasmaCAL standard in demineralized water and measured in triplicate. The range was 0.2 to 2 mg/L for all the metals, with the exception of Fe (0.2 to 10 mg/L), K (2 to 100 mg/L) and Na (2 to 10 mg/L). The R^2 for all elements was always above 0.999 except for Na, which was however always above 0.988. The Relative Standard Deviation (RSD) of the triplicate measurements of the calibration standards was always lower than 1 %, while the ARD with respect to the analyzed standard value was always between 0 and 4 % for all metals except Na. In fact, Na had a higher ARD (always lower than 20 %) which is assumed to be an inherent instrument inaccuracy for Na measurement. High uncertainty in Na concentration by ICP measurements has been reported in literature for fast pyrolysis oil of woody biomass.⁴⁴

2.3.6. Component identification by GC-MS

GC-MS analysis was performed for the identification and quantitation of the GC-detectable fraction (i.e. the volatile fraction) of the bio-crude feed and the extracts. In addition, GC-MS after silylation was performed to identify and quantify free fatty acids and a few phenolic components for which the ion peaks had better resolution than in the non-silylated samples. The analysis was performed on a

255 PerkinElmer Clarus 680 GC coupled with a PerkinElmer Clarus SQ 8T MS. For the analysis of the
 256 feed, the bio-crude was extracted with DEE (bio-crude to solvent ratio approximately 1:50 by mass)
 257 and the resulting DEE-rich mixture was filtered with a syringe filter (pore size 0.45 μm). The amount
 258 of the DEE-soluble fraction of the bio-crude was determined gravimetrically from the filtrate, after
 259 evaporation of the solvent overnight in a fumehood. All sCO_2 extracts were instead fully soluble at a
 260 1:10 extract to DEE ratio (mass basis). GC-MS samples were prepared by mixing approximately 0.1 g
 261 of the DEE-soluble fraction of the feed, or approximately 0.1 g of extract, with approximately 0.7 g a
 262 of a DEE solution containing a known amount of vanillin (1 wt%) as internal standard (IS). Vanillin
 263 was selected as IS as most of the identified components were oxygenated aromatics with some degree
 264 of similarity to vanillin, with vanillin being however not present in the bio-crude samples, not
 265 overlapping with chromatographic peaks of species contained in the bio-crude samples. With regard to
 266 the GC-MS after silylation, the feed and extract samples were silylated as follows: about 0.1 g of each
 267 sample were dried in a heating cabinet for 2 h at 120 $^{\circ}\text{C}$, then diluted in pyridine, which contained a
 268 known amount of myristic acid (1 wt%) as IS, and derivatized with BSTFA at 60 $^{\circ}\text{C}$ for 20 minutes.
 269 Myristic acid was selected as IS as the GC-MS analysis after silylation was aimed at fatty acids, with
 270 myristic acid being however not present in the bio-crude and not overlapping with chromatographic
 271 peaks of species contained in the bio-crude samples. The mixture ratio of sample – pyridine – BSTFA
 272 was 1:1:1 in mass basis. The derivatized samples were further diluted in DEE (1:25 by mass). For all
 273 samples, 1 μl was injected in a PerkinElmer Elite 5 column (30 m, 0.25 mm ID, 0.1 μm), with the
 274 temperature ramping from 40 $^{\circ}\text{C}$ to 250 $^{\circ}\text{C}$ at a rate of 10 $^{\circ}\text{C}/\text{min}$. The initial temperature was held for
 275 3 min while the final temperature was held for 6 min. The injector was maintained at 300 $^{\circ}\text{C}$ and the
 276 helium carrier gas at 1.0 ml/min. The mass fraction of the identified analytes i was calculated as: $w_i =$
 277 $w_{IS} \cdot A_i / A_{IS}$, where A_i and A_{IS} are the chromatographic areas of the analyte i and the IS, respectively,

whereas w_{IS} is the mass fraction of the internal standard (vanillin for pure samples, myristic acid for derivatized samples). Triplicate GC-MS measurements were performed for all samples in random consecution in order to account for random GC response differences.

3. Results and discussion

3.1. Characterization of the feed bio-crude

Table 1 reports the measured bulk properties of the bio-crude feed, including the DEE-soluble fraction, density, TAN, CAN, PhAN, water and metal content. In addition, the elemental carbon (C), hydrogen (H), nitrogen (N) and oxygen (O) mass fractions, as well as the H/C and O/C ratios, are reported on a water-free basis. As can be seen, the density of this bio-crude is approximately 1030 kg/m^3 , which is in line with values reported for HTL bio-crudes from lignocellulosic biomass, reported in the range 970 to 1140 kg/m^3 .^{5,17,20} The TAN value of 97 mg KOH/g is within the values reported in literatures, which range from 30 to 150 mg KOH/g for HTL lignocellulosic bio-crudes.^{5,18,45} With regard to the elemental composition, the mass fractions are also in line with typical woody HTL bio-crudes (i.e. C: 0.76 – 0.84; H: 0.07 – 0.10; N: 0.002 – 0.030; O: 0.05 – 0.15).^{5,7,17,18}

Table 1. Bulk properties at ambient conditions, elemental composition on a water-free basis and metal mass fraction of the feed bio-crude with standard deviations.

Property		Metal content (mg/kg)	
DEE soluble fraction	0.70 ± 0.03	Al	40 ± 9
Density (kg/m^3)	1030 ± 9	Fe	190 ± 20
TAN (mg KOH/g)	97 ± 2	K	3400 ± 400

CAN (mg KOH/g)	42 ± 1	Mg	96 ± 20
PhAN (mg KOH/g)	56 ± 2	Na	3800 ± 500
Water content (wt%)	5.7 ± 0.4	Ti	40 ± 3
C mass fraction	0.80 ± 0.01	Total metals	8500 ± 800
H mass fraction	0.08 ± 0.01		
O mass fraction	0.10 ± 0.02		
N mass fraction	0.017 ± 0.005		
H/C	1.2 ± 0.1		
O/C	0.09 ± 0.02		

294

295 As can be seen in Table 1, the bio-crude exhibits a water content of almost 6 wt%, which is at the lower
296 range of typical reported values for HTL lignocellulosic bio-crudes (i.e. 5 – 15 wt%).^{4,5,7,17} In addition,
297 the bio-crude exhibits a high metal content of around 0.85 wt%, with potassium (K) and sodium (Na)
298 constituting more than 90 % of the total. The metal content is dependent on the biomass ash content,
299 but since woody biomass has typically low ash,⁴⁶ the high metal content mostly originates from the
300 chemicals used in the HTL process. This behaviour was observed by Dénier et al.²¹, who performed
301 HTL of blackcurrant pomace and observed ash contents in the bio-crude increasing (i.e. from 0.1 to 5.3
302 wt%) with sodium hydroxide added (i.e. from 0 to 9 wt%). With regard to Mg, it is known to bind with
303 organic molecules in biomass,⁴⁷ while Al and Fe are typically introduced during the harvest and
304 processing of the biomass.²⁴ Ti is one of the less abundant metals in biomass,⁴⁷ which is assumed to be
305 introduced by equipment wear. The presence of Mg, Al, Fe, Ti, although in relatively small amount
306 (0.03 wt% in total), is confirmed in this work.

307 In total, 46 components were identified by GC-MS in the DEE-soluble fraction of the feed. Detailed list
308 of the components along with retention time (RT), classification, molecular weight (MW), chemical
309 formula, CAS registry number and their mass fraction (wt%) in the feed bio-crude is reported in the
310 supporting information (Table S1). The identified components constitute 19.3 wt% of the feed bio-
311 crude. The unidentified components of this volatile fraction correspond to a chromatographic area that
312 is about twice as large as the identified fraction, which means that, as a rough estimation, about 60 wt%
313 of the bio-crude can be assumed as volatile. The identified components were lumped into 10 categories
314 according to their chemical functionalities: 1) Cyclic aliphatic (C6 – C9) ketones, saturated or
315 monounsaturated (Ketones, K); 2) Alkylbenzenes (AB); 3) Phenol and alkylphenols (Phenols, P); 4)
316 Guaiacol and alkylguaiacols (Guaiacols, G); 5) Benzenediols and acetyl derivatives of benzenediols
317 (BD); 6) 2- and 3-ring aromatic hydrocarbons (PAH); 7) Dehydroabietyl alcohol (ArAl); 8) Short chain
318 fatty acids, in the range C2 – C8 (SFA); 9) Long chain fatty acids, in the range C16 – C18 (LFA); 10)
319 Dehydroabietic acid (ArAcid).

320 The largest fraction of the identified components is constituted by PAHs, which account for 9 wt% of
321 the bio-crude. Even though such components are not often reported often, some have been reported by
322 Pedersen et al.¹⁸ in the distillation residue of woody HTL bio-crude. Retene has been reported in the
323 HTL bio-crude of softwood lignin.⁴⁸ Retene and phenanthrenes are possibly the degradation products
324 of dehydroabietic acid in the biomass, since they are typically found as products of its thermal
325 degradation (e.g. wood smoke).^{49,50}

326 Single-ring aromatic hydrocarbons (alkylbenzenes, AB) are also found, albeit in lower amount (1
327 wt%). Aliphatic hydrocarbons are not observed. Fatty acids (SFA + LFA) are the second most
328 abundant group, accounting for almost 4 wt% of the oil, with the LFA being largely predominant (3.75

wt%). Fatty acids are typically one of the most abundant classes in bio-crudes,⁵¹ although their mass fractions are not often reported. Dehydroabietic acid and dehydroabeytil alcohol are also observed in remarkable amount, 1.8 wt% and 0.4 wt%, respectively. Abietane skeleton diterpenoids are major structures of conifers such as pine,⁵⁰ and dehydroabietic acid is therefore expected to be present in the pine biomass of the bio-crude used in this work. The presence of dehydroabietic acid in the bio-crude suggests that it remains unconverted, to some extent, during the HTL process. Ketones are always present in lignocellulosic bio-crudes. However, even though they are numerous, they are in low amount, summing up to 0.5 wt% of this oil. Single-ring phenolics (alkylphenols, catechols and other types of benzenediols, and guaiacol) account altogether for 2.6 % of the bio-crude. Alkylphenols, catechols and guaiacols are typically observed in HTL of softwood lignin,^{3,14,48} with the ratio catechols to guaiacols increasing with the HTL reaction temperature.^{14,48} Their presence and the low guaiacols/catechols ratio is therefore qualitatively in line with the high-temperature hydrothermal decomposition of the lignin contained in the original biomass of this work.

3.2. Extraction conditions and yields

The experimental conditions and mass balances for each supercritical extraction are reported in Table 2. Four different extraction temperatures (i.e. 80, 100, 120 and 150 °C) were tested at two pressures (i.e. 330 and 450 bar). The lower pressure (330 bar) was chosen to be within the typical pressure range of the HTL process,¹⁹ therefore allowing the investigation of the sCO₂ extraction at pressure levels comparable to the HTL reactor, as higher pressures in the downstream separation would be less favourable for process economics. The higher pressure (450 bar) was selected on the basis of previous works,^{22,37} which showed promising results in terms of attainment of high extraction yields. The duration of the extractions was between 5.3 and 6.4 hours. Table 2 also reports: the density of pure CO₂

at the operating conditions of the extraction (ρ); the average solvent mass flow rate (Q); the mass of feed bio-crude charged in the extractor at the beginning of an experiment (F); the mass of the four extracts collected in each extraction ($E1$, $E2$, $E3$ and $E4$), with the exception of run A where only three extracts were collected. Run A was the extraction with the lowest yield and the third sampling vial (i.e. $E3$) was maintained for a longer period to avoid ending up with $E4$ sample mass inadequate for analysis. The mass balance discrepancy (losses, L) of each run is also reported, together with the total solvent-to-feed ratio (i.e. at the end of the run) and the total extraction yield. The total extraction yield is defined as the ratio of the total mass of the collected extracts to the mass of the feed. It is therefore determined gravimetrically. Data from Table 2 were also used to calculate the Vapour Phase Loading (VPL) as the extractions progress. VPL is defined as the ratio of the mass of extract in a given time interval over the mass of solvent flowed in the same interval. VPL values were also used to evaluate the reproducibility of the extraction procedure. In this regard, six repetitions of Run H were carried out and the RSD on VPLs were found to be: 7.1 % for extract 1 ($E1$); 11.6 % for extract 2 ($E2$); 14.0 % for extract 3 ($E3$); 11.3 % for extract 4 ($E4$).

Table 2: Experimental extraction conditions and results. Temperature (T); pressure (P); CO_2 density (ρ); average CO_2 mass flow rate (Q); mass of feed (F); mass of extract samples ($E1$, $E2$, $E3$, $E4$); mass of residue (R); losses (L); solvent-to-feed ratio (S/F); total yield (Y_T).

Run ID	A	B	C	D	E	F	G	H
T (°C)	80	100	120	150	80	100	120	150
P (bar)	330	330	330	330	450	450	450	450

ρ (kg/m³)^a	773	696	623	531	851	790	731	650
Q (g/min)	5.2	5.5	5.0	4.7	5.7	5.9	5.0	4.8
F (g)	48.9	52.6	51.3	53.6	53.9	51.5	54.2	51.9
E1 (g)	6.6	5.7	7.7	5.4	5.3	8.4	6.9	6.6
E2 (g)	6.1	5.9	5.3	6.9	5.3	5.8	6.4	7.6
E3 (g)	8.9	6.0	5.6	5.0	5.3	5.5	6.9	6.2
E4 (g)	-	6.2	5.0	7.5	8.1	7.2	7.8	7.3
R (g)	23.1	24.4	22.8	23.8	23.9	21.0	22.2	18.0
L (%)	8.2	6.5	9.4	9.0	9.4	7.0	8.5	12.0
S/F (g/g)	30.2	36.5	36.3	31.6	32.4	36.7	33.3	30.0
Y_T (%)	44.1	45.1	46.0	46.3	47.3	52.4	51.5	53.4

^a Taken from NIST ⁴³;

In Table 2, it can be seen that the highest extraction yield of 53.4 % is not achieved at the highest solvent density, but in fact at the highest temperature and in combination with high pressure. This observation highlights the importance of high temperatures for sCO₂ separation of bio-crudes and it is in line with previous works,^{22,37} where extraction yields up to 48.9 % have been achieved at 448 bar and 120 °C while low efficiency and bad operability were observed below 80 °C. Importantly, not only was Run H characterized by the highest yield but also by the lowest S/F (i.e. 30 g/g). These results indicate that operating conditions of the downstream sCO₂ separation at pressures higher than the pressure of the HTL reactor should not be discarded a priori in the design of the process.

In Figure 2, the extraction yield is plotted vs. the solvent to feed ratio at the four different temperatures and the two pressures. In all cases, the effect of pressure is beneficial for the extraction efficiency,

379 showing higher extraction yields at given S/F values. This is a general feature in sCO₂ separation
380 processes, since higher pressures at given temperatures lead to higher solvent density and increased
381 solvent power. The perusal of Figure 2 also shows that the increase in process efficiency with pressure
382 at given temperature is more pronounced at higher temperatures. This is due to the isothermal variation
383 of the solvent density, which is monotonically increasing with temperature, ranging from 78 to 119
384 kg/m³ as temperature increases from 80 to 150 °C. The increase of the yield for given S/F as pressure
385 increases at constant temperature, which is to say the increased extract to solvent ratio (E/S) with
386 pressure, is typically observed in sCO₂ extraction processes. The primary reason is the increase in
387 solubility of extractable species in the supercritical solvent. However, it is recognised that the
388 extraction yield is affected by both the solubility of extractable species and by mass transfer parameters
389 .⁵²

Accepted author manuscript

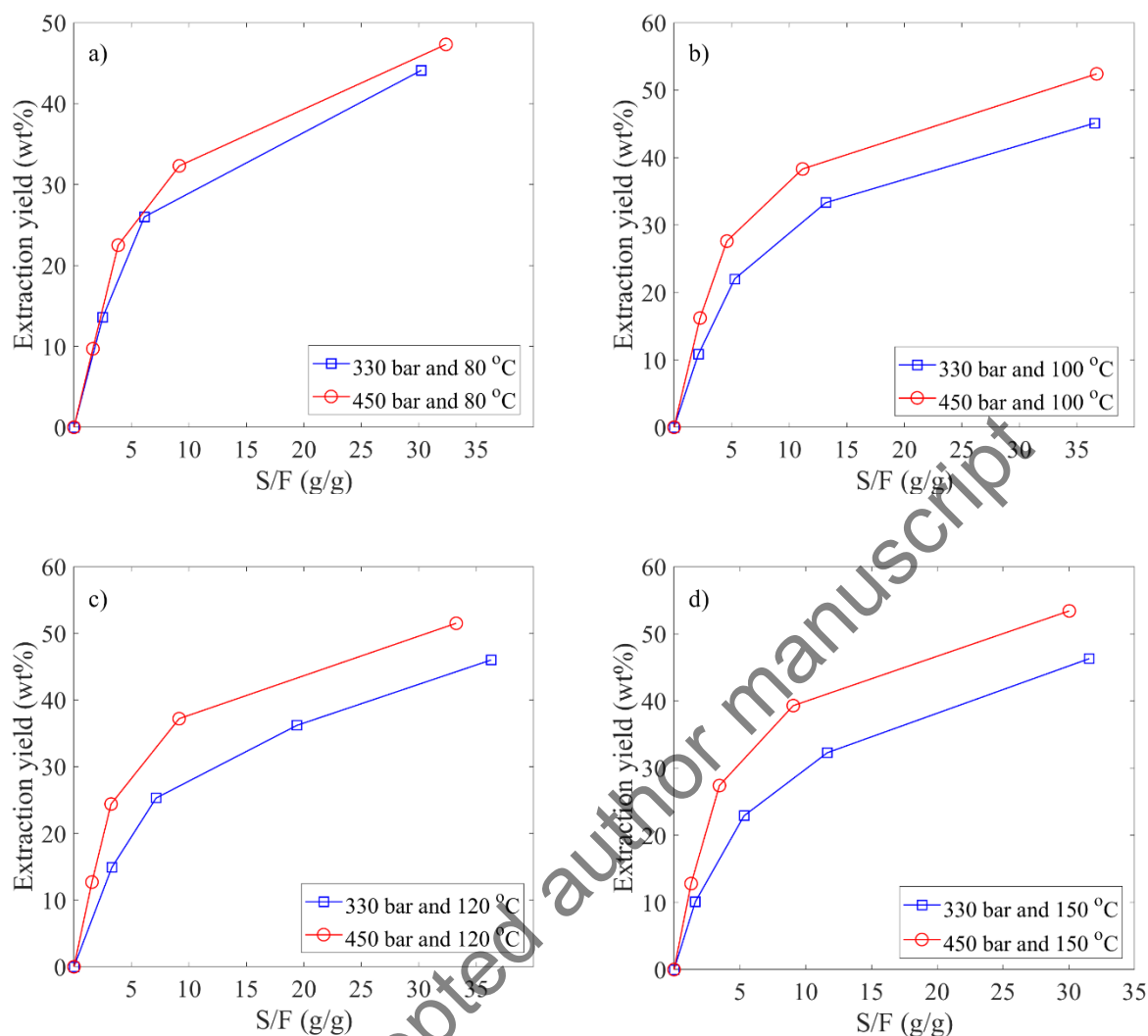


Figure 2. Pressure effect on the extraction yield vs. solvent to feed ratio (S/F) at: a) 80 °C; b) 100 °C; c) 120 °C and d) 150 °C.

In order to visualize this combined effect, Figure 3 shows the extraction yield against S/F at the two studied pressures (i.e. 330 and 450 bar). At 330 bar it is observed that, even though the increase of temperature decreases the solvent density, the extraction yields are comparable for all temperatures. This could indicate that the solubility of the bio-crude at this pressure reduces with temperature, but the mass transfer parameters improve enough to counteract the reducing solubility. Contrary to the

behaviour at 330 bar, at 450 bar the extraction yield slightly increases with temperature. This could be either due to a crossover pressure between 330 and 450 bar that results to solubility increasing with temperature, or due to mass transfer improvements prevailing to the solubility decrease with temperature. Phase equilibrium measurements of the solubility of this type of bio-crude in sCO₂ are not available in the literature and they would be needed to prove the above-mentioned hypotheses.

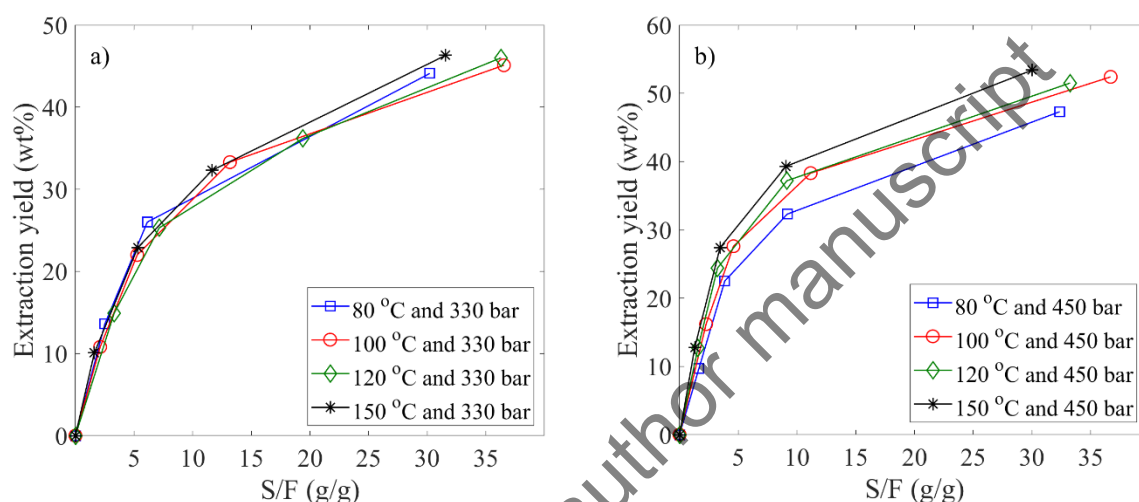


Figure 3. Temperature effect on the extraction yield vs. solvent to feed ratio (S/F) at: a) 330 bar and b) 450 bar.

In theory, the slope of the curves in Figure 2 and Figure 3 (dE/dS) indicates the Vapour Phase Loading (VPL), i.e. the instantaneous value of the mass of components extracted per unit mass of solvent. The collection of a number of extracts per each run allowed to estimate average VPL values ($\Delta E/\Delta S$) as the extraction proceeds. Results are presented for the extractions at 100 °C (Figure 4a) and 150 °C (Figure 4b) and at 330 (Figure 5a) and 450 bar (Figure 5b). Similar trends as Figure 4 are observed at all temperatures studied.

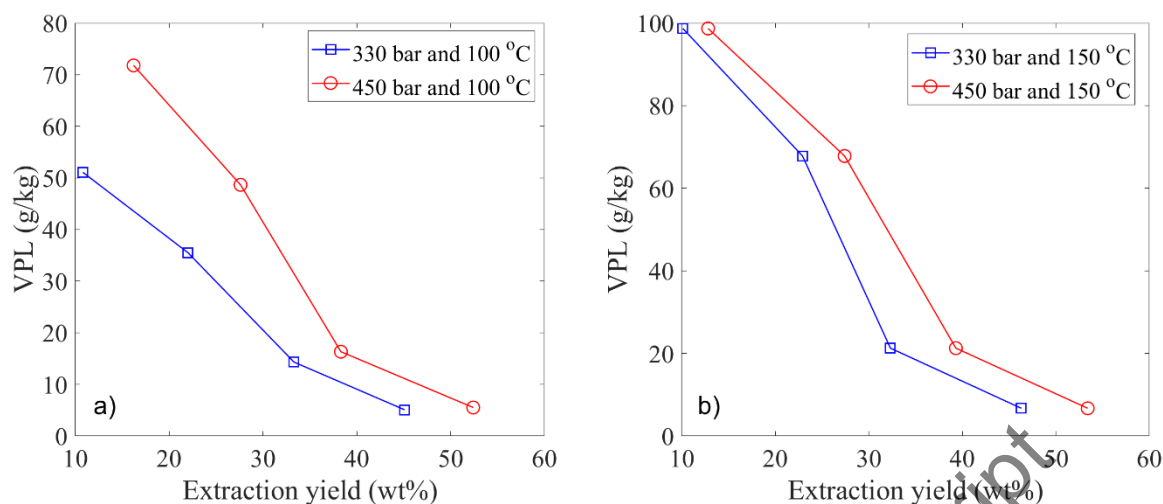


Figure 4. Pressure effect on the vapour phase loading (VPL) vs. extraction yield at: a) 100 °C; b) 150 °C.

As usual, VPL values decrease during the extraction, as the unextracted bio-crude remaining inside the extractor becomes progressively heavier. As can be seen from Figure 4, higher pressure at given temperature leads to higher VPL values, which resulted to the highest extraction yield with the least solvent used in Run H. On the other hand, the effect of temperature is more complex as can be seen in Figure 5. Figure 5b shows that higher temperatures affect positively the VPL at 450 bar, especially in the early stages of the extraction. Whereas at 330 bar (Figure 5a) this effect is only observed at the highest temperature (i.e. 150 °C) and for extraction yields below approximately 30 wt%.

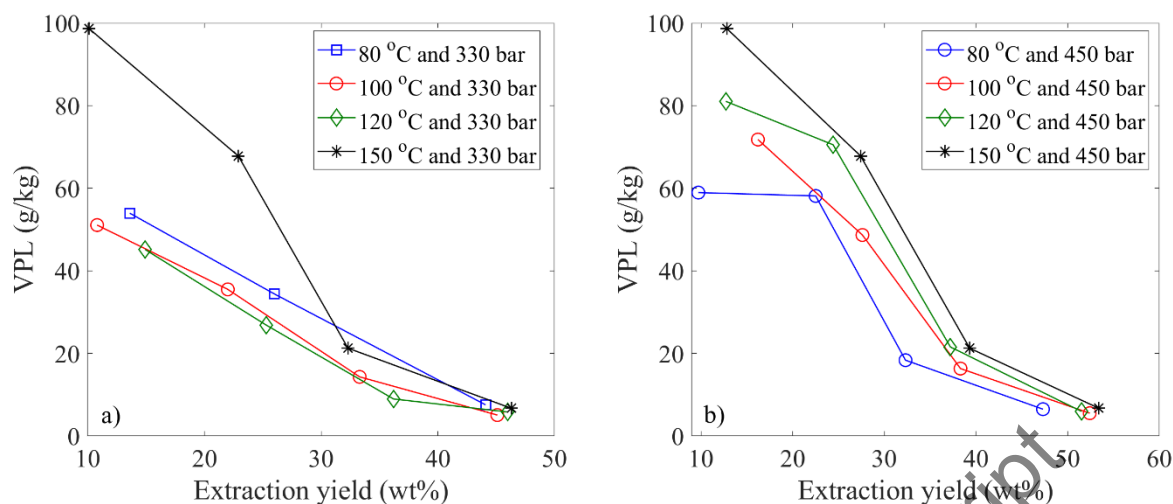


Figure 5. Temperature effect on the vapour phase loading (VPL) vs. extraction yield at: a) 330 bar and b) 450 bar.

An interesting observation arises when the results of this work at 120 °C and 450 bar are compared with an extraction run carried out at basically same conditions (120 °C and 448 bar) on a dewatered bio-crude (water content 2.7 %), presented in a previous work.³⁷ In Figure 6a, the cumulative extract is plotted against S/F for a normalized feed mass (i.e. 50 g). It can be seen that the extraction is more efficient for the non-dewatered bio-crude of this work. The results of this work show an increase of extract in the range 3 to 6 g, for given S/F values ranging from 1.3 to 30. The difference in water content for 50 g of the two bio-crudes is 1.5 g. Considering that the variation of the extract mass is 2 to 4 times higher than the water content in the feed, it is apparent that the increase in the extract cannot be entirely attributed to the extraction of water itself. Therefore, the presence of water actually enhances the extraction of other molecules contained in the bio-crude feed.

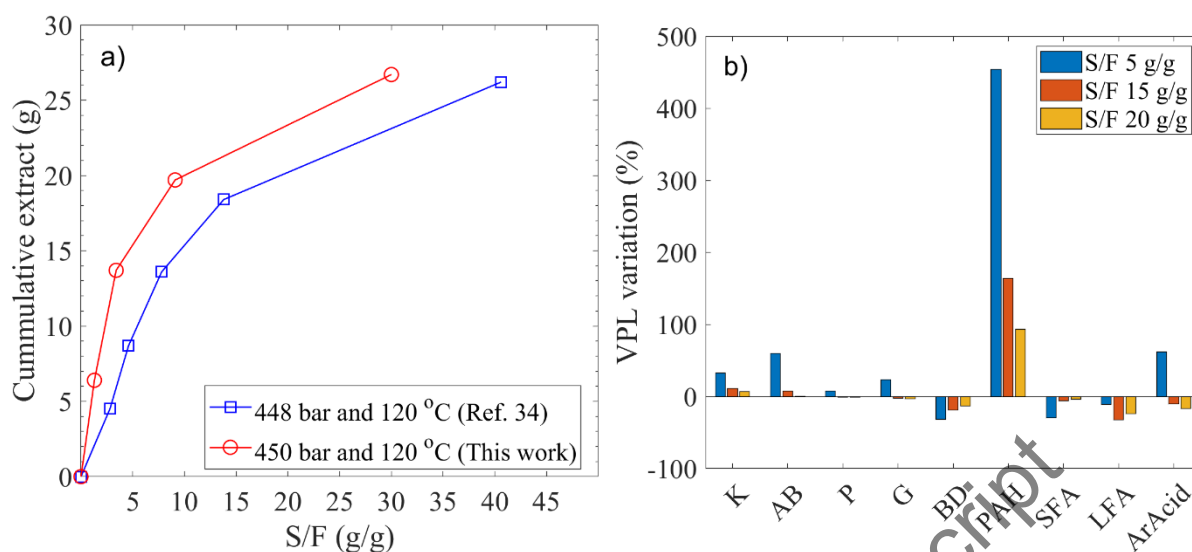


Figure 6. a) Cumulative extract mass (normalized to 50 g feed) vs. S/F for extraction of dewatered bio-crude (2.7 wt% water)³⁷ and the bio-crude of this work (5.7 wt% water); b) Vapour phase loading (VPL) variation of chemical classes between dewatered bio-crude³⁷ and the bio-crude studied in this work. Ketones (K); Alkylbenzenes (AB); Phenols (P); Guaiacols (G); Benzenediols (BD); 2- and 3-ring aromatic hydrocarbons (PAH); Short chain fatty acids, in the range C2 – C8 (SFA); Long chain fatty acids, in the range C16 – C18 (LFA); Dehydroabietic acid (ArAcid).

This enhancement can be discussed in further detail with the aid of Figure 6b, where the variation of VPL, in the two above-mentioned experiments, is shown for specific chemical classes at different S/F ratios. In Figure 6b, nine out of the ten classes defined in this work are represented, since no aromatic alcohols were reported in the previous work. The major observation from Figure 6b is that the higher water content enhances dramatically the VPL of the non-polar hydrocarbons (i.e. AB and PAH). In addition, components of low polarity (e.g. K, P, G) are extracted more efficiently. The more polar components (i.e. BD, SFA and LFA) have in general higher VPL for the bio-crude with the lower initial water content. In all cases the benefit of the presence of water is reduced while the extraction

progresses, which is in line with the slope in the curves of Figure 6a, and suggests that this effect becomes less pronounced as the unextracted residue becomes drier. The above indicates that the application of sCO₂ extraction on the non-dewatered bio-crude leads to both increased VPL and selectivity with respect to polar and apolar components.

3.3. Bulk properties and elemental composition

The values of CAN and PhAN for the extracts increase with the extraction yields (E/F) at all conditions. As an example, the CAN and PhAN values of the extractions at 150 °C are plotted vs. the extraction yield and shown in Figure 7.

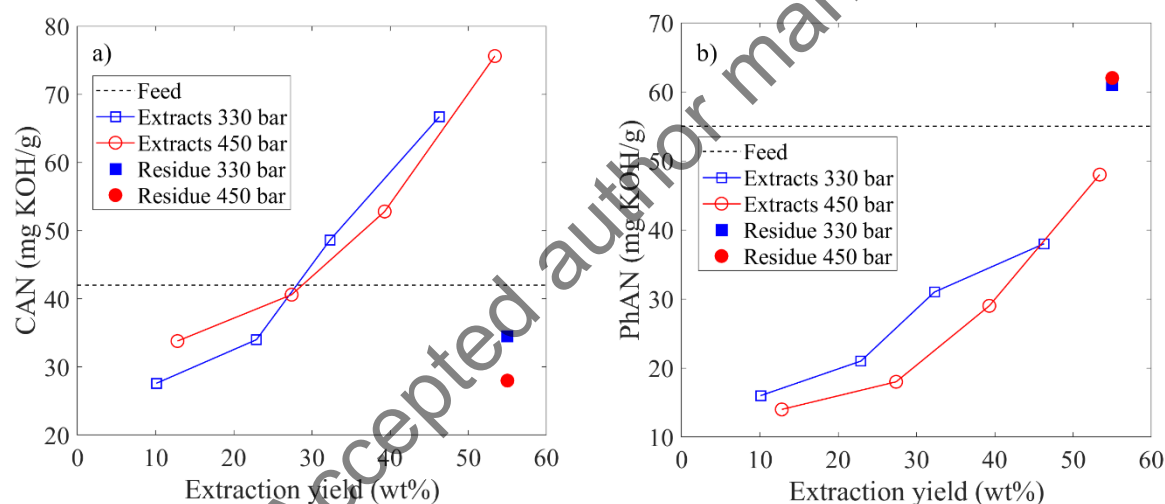


Figure 7. Effect of pressure on a) CAN vs. extraction yield and b) PhAN vs extraction yield at 150 °C

CAN values of the first extracts range from 28 to 41 mg KOH/g, which are values always lower than the CAN value of the feed (42 mg KOH/g). This observation indicates that fatty acids are not preferentially extracted at the beginning of the batch separation process. As the extraction proceeds, the CAN value of the extracts increases, with values ranging from 34 to 41 mg KOH/g for E2, 49 to 53 mg KOH/g for E3 and 67 to 76 for E4 mg KOH/g. The trend of the CAN indicates that fatty acids are

466 progressively more extracted as the extraction proceeds. CAN of the residues ranges from 28 to 35 mg
467 KOH/g, which means that, in most of the cases, the residue is partially depleted of carboxylic acids.
468 When CAN values in this work are compared to those of previous work on a dewatered bio-crude,²² it
469 is observed that in the early stages of the extraction (S/F up to 5 g/g), the literature CAN values are
470 higher (i.e. 37 – 47 mg KOH/g) than those of this work (at similar conditions 80 -120 °C and 255 – 400
471 bar). This further indicates that, at the beginning of the separation process, the fatty acids are less
472 extracted in the presence of higher water content.

473 On the other hand, PhAN values of the extracts are always lower than the value of the feed (55 mg
474 KOH/g). In this case, the values ranges from 14 to 16 mg KOH/g for E1, 18 to 21 mg KOH/g for E2,
475 29 to 31 mg KOH/g for E3 and 38 to 48 mg KOH/g for E4. Consistently, the PhAN value of the
476 residue is higher than the feed, resulting to be in the range 61 to 62 mg KOH/g. Overall, the reduced
477 CAN and increased PhAN in the residue indicates that its type of acidity is shifted towards phenolic
478 nature. The highest value of CAN was observed for extract E4 at 450 bar and 150 °C (i.e. 76 mg
479 KOH/g), while the lowest PhAN was observed for extract E1 for the same extraction (i.e. 14 mg
480 KOH/g). A high CAN and low PhAN is advantageous for hydrotreating since HDO of fatty acids is
481 easier than opening aromatic rings.^{53,54} In addition, the increased PhAN indicates that high molecular
482 weight phenolic components remain in the residue. This fraction is expected to be resistant to HDO, as
483 it was similarly shown for the residue of n-pentane extraction of lignocellulosic bio-crude.⁵⁵

484 The density of the extracts was found in the range of 914 to 1034 kg/m³, increasing with the extraction
485 progression. Most of the sCO₂ extracts exhibit a moderate reduction compared to the feed, with the
486 maximum being a 10 % reduction for early extracts (i.e. E1, E2). The later extracts show a density
487 comparable to the feed, with only the final extracts (i.e. E4) at 80 °C and 300 bar and 100 °C and 450

bar exhibiting a density slightly higher than the feed (see example in Figure 8b). The extraction conditions show negligible influence on the density of the extracts. As in the case of acidity, also in the case of density the trends were similar at all experimental conditions. Figure 8a shows an example referred to the extractions at 150 °C, whereas Figure 8b shows two cases at 450 bar.

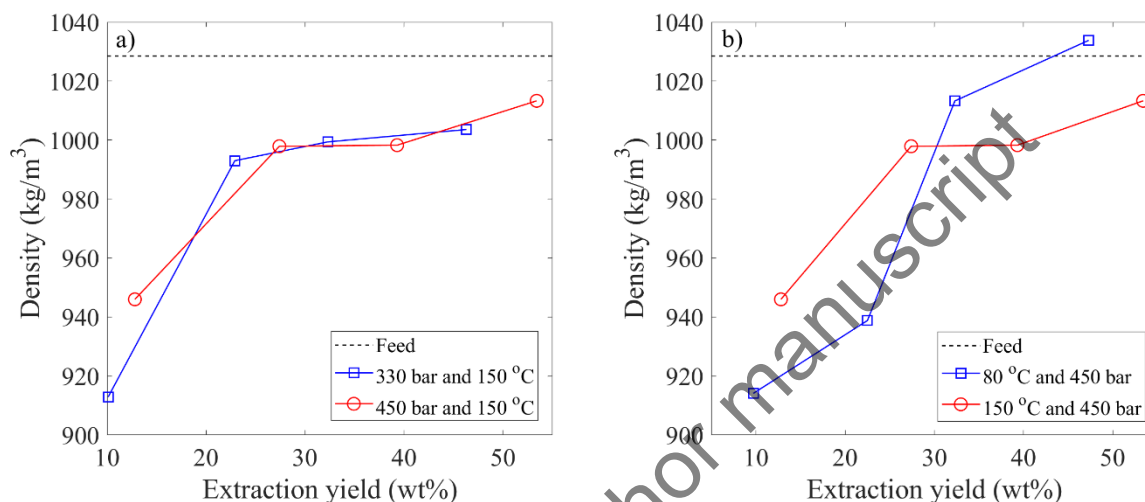


Figure 8. Density vs. extraction yield at: a) Constant temperature (150 °C); b) Constant pressure (450 bar).

The water content of the extracts was measured for the experimental runs B, E, D, and H and resulted to be in the range 1.3 to 1.8 wt%, with no clear trend with the extraction pressure and temperature. Importantly, the values are consistently and remarkably lower than the water content of the feed (i.e. 5.7 wt%). The water content of the residues of the same extractions was measured after evaporation of the solvent used for their recovery. The obtained values were in the range 0.9 to 1.6 wt%. The fact that the water content was observed to decrease both in the residue and in the extract clearly indicates that it was not possible to recover all the water from the system, due to lack of complete recovery in the cold trap and/or water losses during the recovery of the residue at the end of the extraction. The mass

503 balances indicate that approximately 50 % of the water originally in the feed was not retrieved in the
504 extracts and in the residue. For extraction D, the water content of the residue was measured by means
505 of direct KF titration of a sample of THF solution, i.e. before the solvent evaporation. The value was
506 1.2 wt%, while the corresponding value after solvent evaporation was 0.9 wt%. This means that about
507 2% of the water in the feed was lost during the vacuum evaporation, which is not significant with
508 regard to the total water losses. Interestingly, the earlier extracts (i.e. E1, E2) exhibited spontaneous
509 separation of water, with water droplets collecting at the bottom of the storage vials. This was not
510 observed for the later extracts (i.e. E3, E4). This freely separated water was determined for extractions
511 at 150 °C and it was 0.4 g and 0.6 g for extractions H and D, respectively, which corresponds to 13 %
512 and 20 % of the original water in the feed. Even though it was not possible to close the mass balances
513 on water, the results clearly indicate that sCO₂ process co-extracts water from the HTL bio-crude,
514 induce the separation of water from the extracts and allows reducing the water content in the residue as
515 well.

516 The carbon mass fraction in the extracts was in the range 0.80 to 0.81, which are values close to the
517 values of the feed (i.e. 0.80) and the residue (0.78 – 0.79). The hydrogen content (on a water-free basis)
518 is slightly increased in the extracts (0.09 – 0.11), with respect to the feed (i.e. 0.08) and the residues
519 (range 0.07 – 0.08). The oxygen mass fraction of the extracts (on a water-free basis) was for all
520 extractions lower than that of the feed, ranging from 0.05 to 0.07 (vs. 0.10 in the feed). In line with this,
521 the mass fraction of oxygen of the residues increased, ranging from 0.13 and 0.15. The oxygen mass
522 fraction of the extractions performed at 150 °C is plotted in Figure 9 as a function of the extraction
523 yield. Similar trends are observed in all extractions.

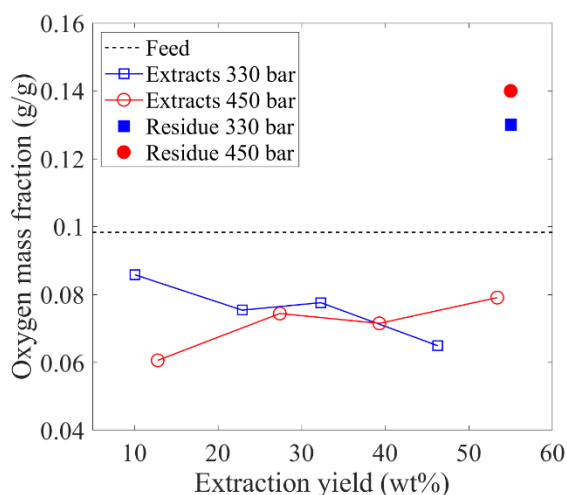


Figure 9. Oxygen content on a water-free basis vs extraction yield for extractions at 150 °C.

3.4. Metal content of bio-crude extracts and residues

The metal content of extracts and residues was measured for extraction B, D, G and H. In all cases, the extracts were found almost completely devoid of metals. The metal content was reduced from 95 % to 99 %, compared to the feed value. The analysis of the residues confirmed that the metals are concentrated in the unextracted phase. The trends were very similar in all runs. As an example, the results obtained with the extraction at 330 bar and 150 °C are reported in Figure 10.

As can be seen in Figure 10, potassium and sodium, which constitute more than 90 % of the metal content of the feed, are reduced from 3400 mg/kg and 3800 mg/kg down to values ranging from 30 to 40 mg/kg and 70 to 100 mg/kg, respectively. Aluminium, iron and titanium are reduced in the extracts down to values below 10 mg/kg in all extracts. Interestingly, magnesium remains unchanged, which suggests that it may be in organometallic components²⁴ that can be solubilized by sCO₂. In all cases, the total metal content was found to be drastically reduced from 8500 mg/kg down to an average value of 170 mg/kg.

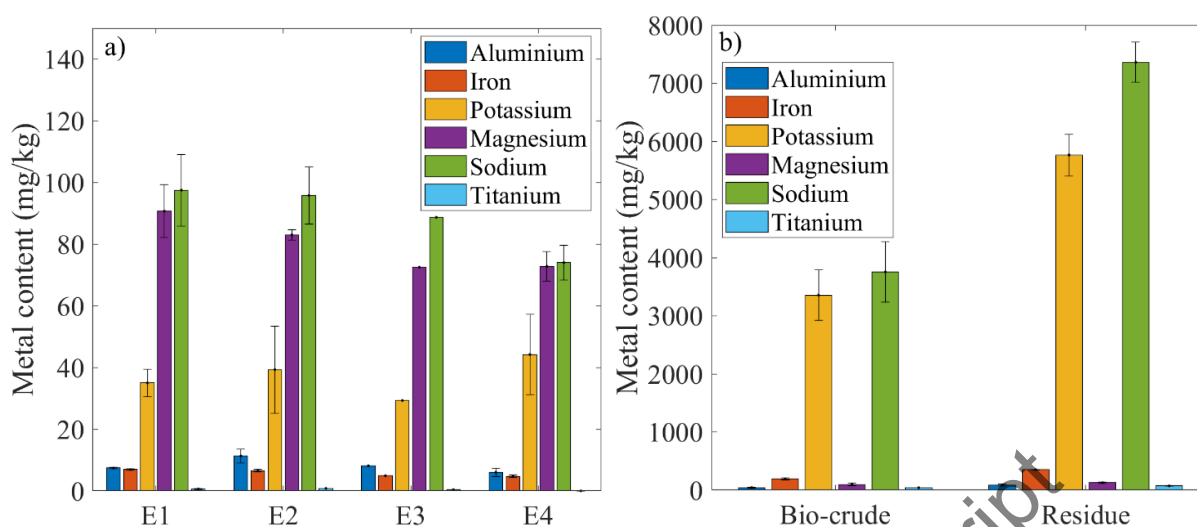


Figure 10: Metal distribution between bio-crude, extracts (i.e. E1, ..., E4) and residue for the extraction at 330 bar and 150 °C. Error bars represent the standard deviation of at least duplicate measurements.

The small amount of metals in the extracts indicates that either they can be entrained together with fine water droplets where they are dissolved in, or they are present, albeit in very small amount, as organometallic components that are soluble in sCO_2 . The 10 μm filter at the top of the basket insert is expected to act as a factor limiting the entrainment of water droplets.

3.5. Chemical composition by GC-MS

Figure 11a shows the total ion chromatograms (normalized with respect to the highest peaks) of the non-derivatized samples of the feed bio-crude and the extracts obtained at 330 bar and 150 °C. Figure 11b shows the corresponding chromatograms for the derivatized (silylated) samples. The trends shown in Figure 11 are qualitatively representative of all extractions carried out in this work. It is noted that some classes of components exhibit overlapping Retention Time (RT) ranges, which does not allow assuming that all components in a certain RT range are expected to belong to a specific class. As can be seen in Figure 11a, the concentration of lower retention time components (up to 17 min) is increased in

the first extract, while it decreases in subsequent extracts. This indicates that these components are preferentially extracted at the beginning of the process and depleted in the unextracted oil. The peak areas of higher retention time components (21 – 25 min) increase over time, which is particularly visible by the increasing difference between the largest peak of the chromatograms (retene at 23.8 min) and the IS (vanillin at 15.1 min). This indicates that they are not preferentially extracted in the early stages of the extraction, but are substantially extracted as their concentration in the residue increases. Similar trend is observed in the derivatized sample (Figure 11b), with light components (RT up to 15 min) extracted preferentially in the early stages while gradually depleted. In this case, the heavy acids (i.e. LFA and ArAcid, RT above 21 min) are progressively extracted in relatively higher amounts as the extraction proceeds.

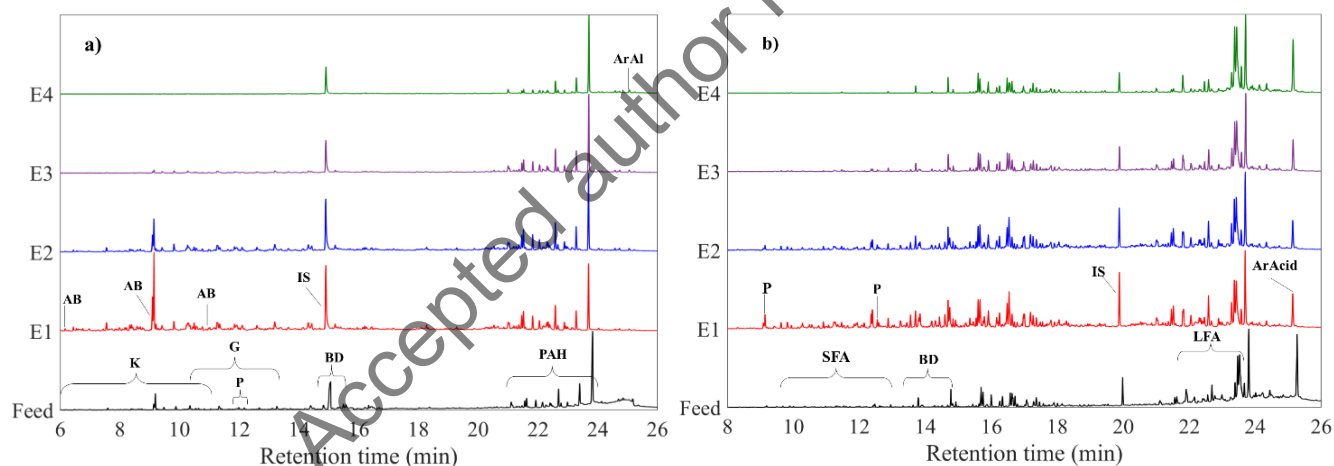


Figure 11. Chromatograms of feed bio-crude and extracts E1 – E4 of the extraction at 330 bar and 150 °C. a) non-derivatized samples; b) derivatized (silylated) samples. Ketones (K); Alkylbenzenes (AB); Phenols (P); Guaiacols (G); Benzenediols (BD); 2- and 3-ring aromatic hydrocarbons (PAH); Aromatic alcohol (ArAl); Short chain fatty acids, in the range C2 – C8 (SFA); Long chain fatty acids, in the range C16 – C18 (LFA); Dehydroabietic acid (ArAcid).

570 Figure 12 shows the progress of the mass fractions of the identified classes of components with the
571 extraction time with reference to the extractions at 150 °C, which are taken as a representative example
572 of all extractions. The total identified components in the sCO₂ extracts are in the range 27 wt% to 40
573 wt%, which are higher values compared to the feed (19 wt%). This observation, together with the
574 reduction in density (see Section 3.3) indicate that the extract has lower average molecular weight than
575 the feed. A lower average molecular weight is expected to reduce coking during catalytic
576 hydrotreatment, thus prolonging the lifecycle of the catalyst.²⁵

577 Ketones, alkylbenzenes, phenols, guaiacols and short chain fatty acids are decreasing monotonically
578 with extraction progression, while benzenediols, polyaromatic hydrocarbons, long chain fatty acids and
579 the aromatic acid increase. The aromatic alcohol does not show any specific trend mostly being
580 unchanged between the extracts. In further detail, the mass fractions of the above-mentioned species in
581 the extracts were found in the ranges of: ketones (0.06 – 1.9 wt%); alkylbenzenes (0.05 – 6.6 wt%);
582 phenols (0.03 – 0.9 wt%); guaiacols (0.04 – 2.5 wt%); benzenediols (0.8 – 3.6 wt%); polyaromatic
583 hydrocarbons (8 – 23 wt%); dehydroabetyl alcohol (0.1 – 1.4 wt%); short chain fatty acids (0.09 – 0.3
584 wt%); long chain fatty acids (3 – 14 wt%); dehydroabietic acid (0.8 – 6 wt%).

585

586

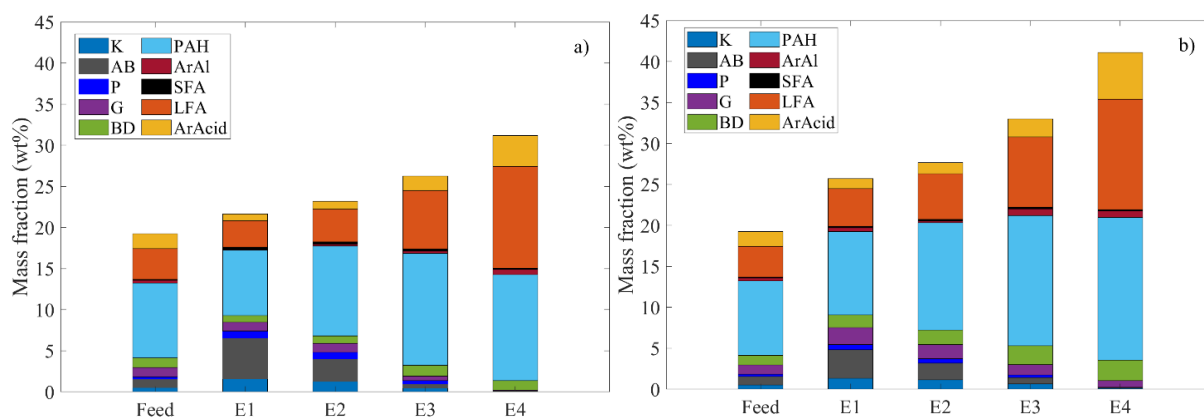


Figure 12. Mass fractions on a water-free basis of the feed and sCO₂ extracts for the experimental runs at: a) 330 bar and 150 °C; b) 450 bar and 150 °C. Ketones (K); Alkylbenzenes (AB); Phenols (P); Guaiacols (G); Benzenediols (BD); 2- and 3-ring aromatic hydrocarbons (PAH); Aromatic alcohol (ArAl); Short chain fatty acids, in the range C₂ – C₈ (SFA); Long chain fatty acids, in the range C₁₆ – C₁₈ (LFA); Dehydroabietic acid (ArAcid).

Overall, the GC-MS analysis shows that the trend of the separation is mainly determined by molecular weight, with the lighter components preferentially extracted in the early stages of the extraction. The polarity plays however an important role as well, as can be observed by the different behaviour between guaiacols, preferentially extracted in the early stages, and benzenediols, which are more polar and are extracted at later stages even though having a slightly lower molecular weight.

4. Conclusion

This work proves that sCO₂ extraction is an effective process for the separation of raw (i.e. non-dewatered and non-demetalized) HTL lignocellulosic bio-crude. The process is capable of extracting a large fraction of the bio-crude (yields of extract up to 53 wt%) with relatively low solvent-to-feed ratios (i.e. 30 to 37 g/g) compared to typical values for sCO₂ extractions. The extracts showed favorable

603 properties towards downstream catalytic hydrotreatment. More specifically, they were drastically
604 demetalized (from 8500 mg/kg down to 170 mg/kg on average), substantially dewatered (from 6 wt%
605 down to 1.3 wt% – 1.8 wt%), exhibited lower oxygen content (from 30 to 50 % reduction on a water-
606 free basis), lower average molecular weight and their acidity was shifted towards carboxylic nature,
607 with a reduction of the phenolic acidity. Interestingly, not only is the sCO₂ process capable of
608 simultaneous demetalization, dewatering and upgrading of the bio-crude, but also the process
609 efficiency was improved, compared to sCO₂ extractions at similar conditions on a dewatered bio-crude.
610 Overall, these properties are expected to lead to longer catalyst life, lower hydrogen requirements and
611 less coking. Experimental studies on hydrotreatment of sCO₂ extracts are needed to confirm the
612 expectations and to provide data allowing to evaluate if the advantages that can be obtained in the
613 hydrotreatment step prevail on the reduced yield of hydrotreatment feed with respect to the initial
614 biomass.

615 Supporting information: List of GC-MS identified components (Table S1)

616 Acknowledgments

617 The authors would like to acknowledge the valuable contribution of Linda Birkebæk Madsen, for
618 performing the elemental analysis for this work.

619

620 References

- 621 (1) Castello, D.; Pedersen, T.; Rosendahl, L. Continuous Hydrothermal Liquefaction of Biomass: A Critical
622 Review. *Energies* **2018**, *11*, 3165. <https://doi.org/10.3390/en11113165>.
- 623 (2) Kim, J. Y.; Lee, H. W.; Lee, S. M.; Jae, J.; Park, Y. K. Overview of the Recent Advances in
624 Lignocellulose Liquefaction for Producing Biofuels, Bio-Based Materials and Chemicals. *Bioresour.*
625 *Technol.* **2019**, *279*, 373–384. <https://doi.org/10.1016/j.biortech.2019.01.055>.
- 626 (3) Nguyen, T. D. H.; Maschietti, M.; Belkheiri, T.; Åmand, L. E.; Theliander, H.; Vamling, L.; Olausson,
627 L.; Andersson, S. I. Catalytic Depolymerisation and Conversion of Kraft Lignin into Liquid Products
628 Using Near-Critical Water. *J. Supercrit. Fluids* **2014**, *86*, 67–75.
629 <https://doi.org/10.1016/j.supflu.2013.11.022>.
- 630 (4) Pedersen, T. H.; Grigoras, I. F.; Hoffmann, J.; Toor, S. S.; Daraban, I. M.; Jensen, C. U.; Iversen, S. B.;
631 Madsen, R. B.; Glasius, M.; Arturi, K. R.; et al. Continuous Hydrothermal Co-Liquefaction of Aspen
632 Wood and Glycerol with Water Phase Recirculation. *Appl. Energy* **2016**, *162*, 1034–1041.
633 <https://doi.org/10.1016/j.apenergy.2015.10.165>.
- 634 (5) Jarvis, J. M.; Billing, J. M.; Hallen, R. T.; Schmidt, A. J.; Schaub, T. M. Hydrothermal Liquefaction
635 Biocrude Compositions Compared to Petroleum Crude and Shale Oil. *Energy and Fuels* **2017**, *31*, 2896–
636 2906. <https://doi.org/10.1021/acs.energyfuels.6b03022>.
- 637 (6) Jensen, C. U.; Rodriguez Guerrero, J. K.; Karatzos, S.; Olofsson, G.; Iversen, S. B. Fundamentals of
638 Hydrofaction™: Renewable Crude Oil from Woody Biomass. *Biomass Convers. Biorefinery* **2017**, *7*,
639 495–509. <https://doi.org/10.1007/s13399-017-0248-8>.
- 640 (7) Jensen, C. U.; Rosendahl, L. A.; Olofsson, G. Impact of Nitrogenous Alkaline Agent on Continuous HTL
641 of Lignocellulosic Biomass and Biocrude Upgrading. *Fuel Process. Technol.* **2017**, *159*, 376–385.
642 <https://doi.org/10.1016/j.fuproc.2016.12.022>.

- 643 (8) Cao, L.; Zhang, C.; Chen, H.; Tsang, D. C. W.; Luo, G.; Zhang, S.; Chen, J. Hydrothermal Liquefaction
644 of Agricultural and Forestry Wastes: State-of-the-Art Review and Future Prospects. *Bioresour. Technol.*
645 **2017**, *245*, 1184–1193. <https://doi.org/10.1016/j.biortech.2017.08.196>.
- 646 (9) Ong, B. H. Y.; Walmsley, T. G.; Atkins, M. J.; Walmsley, M. R. W. Hydrothermal Liquefaction of
647 Radiata Pine with Kraft Black Liquor for Integrated Biofuel Production. *J. Clean. Prod.* **2018**, *199*, 737–
648 750. <https://doi.org/10.1016/j.jclepro.2018.07.218>.
- 649 (10) Jarvis, J. M.; Albrecht, K. O.; Billing, J. M.; Schmidt, A. J.; Hallen, R. T.; Schaub, T. M. Assessment of
650 Hydrotreatment for Hydrothermal Liquefaction Biocrudes from Sewage Sludge, Microalgae, and Pine
651 Feedstocks. *Energy and Fuels* **2018**, *32*, 8483–8493. <https://doi.org/10.1021/acs.energyfuels.8b01445>.
- 652 (11) Belkheiri, T.; Andersson, S. I.; Mattsson, C.; Olausson, L.; Theliander, H.; Vamling, L. Hydrothermal
653 Liquefaction of Kraft Lignin in Sub-Critical Water: The Influence of the Sodium and Potassium Fraction.
654 *Biomass Convers. Biorefinery* **2018**, *8*, 585–595. <https://doi.org/10.1007/s13399-018-0307-9>.
- 655 (12) Anastasakis, K.; Biller, P.; Madsen, R. B.; Glasius, M.; Johannsen, I. Continuous Hydrothermal
656 Liquefaction of Biomass in a Novel Pilot Plant with Heat Recovery and Hydraulic Oscillation. *Energies*
657 **2018**, *11*, 1–23. <https://doi.org/10.3390/en11102695>.
- 658 (13) Sintamarean, I. M.; Grigoras, I. F.; Jensen, C. U.; Toor, S. S.; Pedersen, T. H.; Rosendahl, L. A. Two-
659 Stage Alkaline Hydrothermal Liquefaction of Wood to Biocrude in a Continuous Bench-Scale System.
660 *Biomass Convers. Biorefinery* **2017**, *7*, 425–435. <https://doi.org/10.1007/s13399-017-0247-9>.
- 661 (14) Arturi, K. R.; Strandgaard, M.; Nielsen, R. P.; Søgaard, E. G.; Maschietti, M. Hydrothermal Liquefaction
662 of Lignin in Near-Critical Water in a New Batch Reactor: Influence of Phenol and Temperature. *J.*
663 *Supercrit. Fluids* **2017**, *123*, 28–39. <https://doi.org/10.1016/j.supflu.2016.12.015>.
- 664 (15) Nguyen Lyckeskog, H.; Mattsson, C.; Åmand, L. E.; Olausson, L.; Andersson, S. I.; Vamling, L.;

- Theliander, H. Storage Stability of Bio-Oils Derived from the Catalytic Conversion of Softwood Kraft Lignin in Subcritical Water. *Energy and Fuels* **2016**, *30*, 3097–3106.
<https://doi.org/10.1021/acs.energyfuels.6b00087>.
- (16) Lyckeskog, H. N.; Mattsson, C.; Olausson, L.; Andersson, S. I.; Vamling, L.; Theliander, H. Thermal Stability of Low and High Mw Fractions of Bio-Oil Derived from Lignin Conversion in Subcritical Water. *Biomass Convers. Biorefinery* **2017**, *7*, 401–414. <https://doi.org/10.1007/s13399-016-0228-4>.
- (17) Hoffmann, J.; Jensen, C. U.; Rosendahl, L. A. Co-Processing Potential of HTL Bio-Crude at Petroleum Refineries – Part 1: Fractional Distillation and Characterization. *Fuel* **2016**, *165*, 526–535.
<https://doi.org/10.1016/j.fuel.2015.10.094>.
- (18) Pedersen, T. H.; Jensen, C. U.; Sandström, L.; Rosendahl, L. A. Full Characterization of Compounds Obtained from Fractional Distillation and Upgrading of a HTL Biocrude. *Appl. Energy* **2017**, *202*, 408–419. <https://doi.org/10.1016/j.apenergy.2017.05.167>.
- (19) Ramirez, J. A.; Brown, R. J.; Rainey, T. J. A Review of Hydrothermal Liquefaction Bio-Crude Properties and Prospects for Upgrading to Transportation Fuels. *Energies* **2015**, *8*, 6765–6794.
<https://doi.org/10.3390/en8076765>.
- (20) Haarlemmer, G.; Guizani, C.; Anouti, S.; Déniel, M.; Roubaud, A.; Valin, S. Analysis and Comparison of Bio-Oils Obtained by Hydrothermal Liquefaction and Fast Pyrolysis of Beech Wood. *Fuel* **2016**, *174*, 180–188. <https://doi.org/10.1016/j.fuel.2016.01.082>.
- (21) Déniel, M.; Haarlemmer, G.; Roubaud, A.; Weiss-Hortala, E.; Fages, J. Optimisation of Bio-Oil Production by Hydrothermal Liquefaction of Agro-Industrial Residues: Blackcurrant Pomace (*Ribes Nigrum* L.) as an Example. *Biomass and Bioenergy* **2016**, *95*, 273–285.
<https://doi.org/10.1016/j.biombioe.2016.10.012>.

- 687 (22) Montesantos, N.; Pedersen, T. H.; Nielsen, R. P.; Rosendahl, L.; Maschietti, M. Supercritical Carbon
688 Dioxide Fractionation of Bio-Crude Produced by Hydrothermal Liquefaction of Pinewood. *J. Supercrit.*
689 *Fluids* **2019**, *149*, 97–109. <https://doi.org/10.1016/j.supflu.2019.04.001>.
- 690 (23) Elliott, D. C. Historical Developments in Hydroprocessing Bio-Oils. *Energy and Fuels* **2007**, *21*, 1792–
691 1815. <https://doi.org/10.1021/ef070044u>.
- 692 (24) Leijenhurst, E. J.; Wolters, W.; Van De Beld, L.; Prins, W. Inorganic Element Transfer from Biomass to
693 Fast Pyrolysis Oil: Review and Experiments. *Fuel Process. Technol.* **2016**, *149*, 96–111.
694 <https://doi.org/10.1016/j.fuproc.2016.03.026>.
- 695 (25) Furimsky, E.; Massoth, F. E. Deactivation of Hydroprocessing Catalysts. *Catal. Today* **1999**, *52*, 381–
696 495. [https://doi.org/10.1016/S0920-5861\(99\)00096-6](https://doi.org/10.1016/S0920-5861(99)00096-6).
- 697 (26) Eijssbouts, S.; Battiston, A. A.; van Leerdam, G. C. Life Cycle of Hydroprocessing Catalysts and Total
698 Catalyst Management. *Catal. Today* **2008**, *130*, 361–373. <https://doi.org/10.1016/j.cattod.2007.10.112>.
- 699 (27) ASTM International. ASTM D1655-19a, Standard Specification for Aviation Turbine Fuels. West
700 Conshohocken, PA 2019. <https://doi.org/10.1520/D1655-19A>.
- 701 (28) European Committee for Standardization. EN590:2013+A1 Automotive Fuels -Diesel -Requirements and
702 Test Methods. 2017.
- 703 (29) ISO 8217:2017, Petroleum Products — Fuels (Class F) — Specifications of Marine Fuels. 2017.
- 704 (30) Brunner, G. Counter-Current Separations. *J. Supercrit. Fluids* **2009**, *47*, 574–582.
705 <https://doi.org/10.1016/j.supflu.2008.09.022>.
- 706 (31) Nielsen, R. P.; Valsecchi, R.; Strandgaard, M.; Maschietti, M. Experimental Study on Fluid Phase
707 Equilibria of Hydroxyl-Terminated Perfluoropolyether Oligomers and Supercritical Carbon Dioxide. *J.*
708 *Supercrit. Fluids* **2015**, *101*, 124–130. <https://doi.org/10.1016/j.supflu.2015.03.011>.

- 709 (32) Riha, V.; Brunner, G. Separation of Fish Oil Ethyl Esters with Supercritical Carbon Dioxide. *J. Supercrit.*
710 *Fluids* **2000**, *17*, 55–64. [https://doi.org/10.1016/S0896-8446\(99\)00038-8](https://doi.org/10.1016/S0896-8446(99)00038-8).
- 711 (33) Gironi, F.; Maschietti, M. Separation of Fish Oils Ethyl Esters by Means of Supercritical Carbon
712 Dioxide: Thermodynamic Analysis and Process Modelling. *Chem. Eng. Sci.* **2006**, *61*, 5114–5126.
713 <https://doi.org/10.1016/j.ces.2006.03.041>.
- 714 (34) Dunford, N. T.; Teel, J. A.; King, J. W. A Continuous Countercurrent Supercritical Fluid Deacidification
715 Process for Phytosterol Ester Fortification in Rice Bran Oil. *Food Res. Int.* **2003**, *36*, 175–181.
716 [https://doi.org/10.1016/S0963-9969\(02\)00134-5](https://doi.org/10.1016/S0963-9969(02)00134-5).
- 717 (35) Eisenmenger, M.; Dunford, N. T.; Eller, F.; Taylor, S.; Martinez, J. Pilot-Scale Supercritical Carbon
718 Dioxide Extraction and Fractionation of Wheat Germ Oil. *JAOCS, J. Am. Oil Chem. Soc.* **2006**, *83*, 863–
719 868. <https://doi.org/10.1007/s11746-006-5038-6>.
- 720 (36) Vázquez, L.; Torres, C. F.; Fornari, T.; Señoráns, F. J.; Reglero, G. Recovery of Squalene from
721 Vegetable Oil Sources Using Countercurrent Supercritical Carbon Dioxide Extraction. *J. Supercrit.*
722 *Fluids* **2007**, *40*, 59–66. <https://doi.org/10.1016/j.supflu.2006.04.012>.
- 723 (37) Montesantos, N.; Pedersen, T. H.; Nielsen, R. P.; Rosendahl, L. A.; Maschietti, M. High-Temperature
724 Extraction of Lignocellulosic Bio-Crude by Supercritical Carbon Dioxide. *Chem. Eng. Trans.* **2019**, *74*,
725 799–804. <https://doi.org/10.3303/CET1974134>.
- 726 (38) Jensen, C. U. PIUS – Hydrofaction™ Platform with Integrated Upgrading Step, PhD Thesis, Aalborg
727 University, 2018.
- 728 (39) Patel, R. N.; Bandyopadhyay, S.; Ganesh, A. Extraction of Cardanol and Phenol from Bio-Oils Obtained
729 through Vacuum Pyrolysis of Biomass Using Supercritical Fluid Extraction. *Energy* **2011**, *36*, 1535–
730 1542. <https://doi.org/10.1016/j.energy.2011.01.009>.

- 731 (40) Feng, Y.; Meier, D. Supercritical Carbon Dioxide Extraction of Fast Pyrolysis Oil from Softwood. *J.*
732 *Supercrit. Fluids* **2017**, *128*, 6–17. <https://doi.org/10.1016/j.supflu.2017.04.010>.
- 733 (41) Feng, Y.; Meier, D. Extraction of Value-Added Chemicals from Pyrolysis Liquids with Supercritical
734 Carbon Dioxide. *J. Anal. Appl. Pyrolysis* **2015**, *113*, 174–185. <https://doi.org/10.1016/j.jaap.2014.12.009>.
- 735 (42) ASTM International. *ASTM D664-17a, Standard Test Method for Acid Number of Petroleum Products by*
736 *Potentiometric Titration*; West Conshohocken, PA, 2017. <https://doi.org/10.1520/D0664-17A>.
- 737 (43) Lemmon, E. W.; McLinden, M. O.; Friend, D. G. Thermophysical Properties of Fluid Systems. In *NIST*
738 *Chemistry WebBook, NIST Standard Reference Database Number 69*; Linstrom, P. J., Mallard, W. G.,
739 Eds.; National Institute of Standards and Technology: Gaithersburg MD, 20899.
740 <https://doi.org/https://doi.org/10.18434/T4D303>.
- 741 (44) Oasmaa, A.; Van De Beld, B.; Saari, P.; Elliott, D. C.; Solantausta, Y. Norms, Standards, and Legislation
742 for Fast Pyrolysis Bio-Oils from Lignocellulosic Biomass. *Energy and Fuels* **2015**, *29*, 2471–2484.
743 <https://doi.org/10.1021/acs.energyfuels.5b00026>.
- 744 (45) Madsen, R. B.; Bernberg, R. Z. K.; Biller, P.; Becker, J.; Iversen, B. B.; Glasius, M. Hydrothermal Co-
745 Liquefaction of Biomasses – Quantitative Analysis of Bio-Crude and Aqueous Phase Composition.
746 *Sustain. Energy Fuels* **2017**, *1*, 789–805. <https://doi.org/10.1039/C7SE00104E>.
- 747 (46) Rowell, R.; Pettersen, R.; Tshabalala, M. Cell Wall Chemistry. In *Handbook of Wood Chemistry and*
748 *Wood Composites, Second Edition*; Rowell, R. M., Ed.; CRC Press, 2012; pp 33–72.
749 <https://doi.org/10.1201/b12487-5>.
- 750 (47) Vassilev, S. V.; Baxter, D.; Andersen, L. K.; Vassileva, C. G.; Morgan, T. J. An Overview of the Organic
751 and Inorganic Phase Composition of Biomass. *Fuel* **2012**, *94*, 1–33.
752 <https://doi.org/10.1016/j.fuel.2011.09.030>.

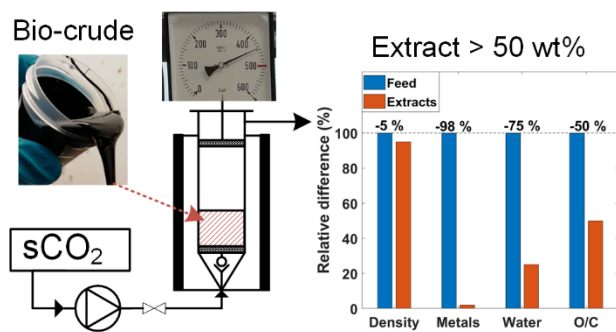
- (48) Nguyen, T. D. H.; Maschietti, M.; Åmand, L. E.; Vamling, L.; Olausson, L.; Andersson, S. I.; Theliander, H. The Effect of Temperature on the Catalytic Conversion of Kraft Lignin Using Near-Critical Water. *Bioresour. Technol.* **2014**, *170*, 196–203. <https://doi.org/10.1016/j.biortech.2014.06.051>.
- (49) Standley, L. J.; Simoneit, B. R. T. Resin Diterpenoids as Tracers for Biomass Combustion Aerosols. *J. Atmos. Chem.* **1994**, *18*, 1–15. <https://doi.org/10.1007/BF00694371>.
- (50) Carpy, A.; Marchand-Geneste, N. Molecular Characterization of Retene Derivatives Obtained by Thermal Treatment of Abietane Skeleton Diterpenoids. *J. Mol. Struct. THEOCHEM* **2003**, *635*, 45–53. [https://doi.org/10.1016/S0166-1280\(03\)00400-7](https://doi.org/10.1016/S0166-1280(03)00400-7).
- (51) Madsen, R. B.; Zhang, H.; Biller, P.; Goldstein, A. H.; Glasius, M. Characterizing Semivolatile Organic Compounds of Biocrude from Hydrothermal Liquefaction of Biomass. *Energy and Fuels* **2017**, *31*, 4122–4134. <https://doi.org/10.1021/acs.energyfuels.7b00160>.
- (52) McHugh, M. A.; Krukonis, V. J. Phase Diagrams for Supercritical Fluid–Solute Mixtures. In *Supercritical Fluid Extraction*; Brenner, H., Ed.; Elsevier, 1994; pp 27–84. <https://doi.org/10.1016/B978-0-08-051817-6.50006-0>.
- (53) Kokayeff, P.; Zink, S.; Roxas, P. Hydrotreating in Petroleum Processing. In *Handbook of Petroleum Processing*; Treese, S. A., Pujadó, P. R., Jones, D. S. J., Eds.; Springer International Publishing, 1995; pp 363–434.
- (54) Mortensen, P. M.; Grunwaldt, J. D.; Jensen, P. A.; Knudsen, K. G.; Jensen, A. D. A Review of Catalytic Upgrading of Bio-Oil to Engine Fuels. *Appl. Catal. A Gen.* **2011**, *407*, 1–19. <https://doi.org/10.1016/j.apcata.2011.08.046>.
- (55) Bjelić, S.; Yu, J.; Iversen, B. B.; Glasius, M.; Biller, P. Detailed Investigation into the Asphaltene Fraction of Hydrothermal Liquefaction Derived Bio-Crude and Hydrotreated Bio-Crudes. *Energy and*

775 *Fuels* **2018**, 32, 3579–3587. <https://doi.org/10.1021/acs.energyfuels.7b04119>.

776

777

Accepted author manuscript



Accepted author manuscript